

A Second-Order Regularization Method of Object Reconstruction in Hydrodynamic Experiments

LingHai Kong, HaiBo Xu

Institute of Applied Physics and Computational Mathematics

Beijing, PR China

email: {kong_linghai, xu_haibo}@iapcm.ac.cn

Abstract— A new higher-order regularization model is investigated under the assumption of mixed Laplace-Gaussian noise, which plays an important role in tomography reconstruction and quantitative analysis of hydrodynamic experiments. To solve the model numerically, adaptive stopping functions are introduced to improve the classical augmented Lagrangian method, and an adaptive soft-shrinking formula is derived. To acquire efficiency and reliability, it is further combined with a variant of the expectation maximization method. Some experimental tests are performed for image denoising and object reconstruction.

Keywords- Regularization Method; Mixed Laplace-Gaussian Noise; ALM; EM; Image Reconstruction.

I. INTRODUCTION

Image reconstruction is an indispensable process in image processing and data analysis, whose goal is to rebuild an ideal image from noisy or even blurred data. Some different types of mixed noise models have been investigated in the literature, such as Poisson and Gaussian noise [1][2], impulse and Gaussian noise [3]-[5], etc.. With regards to impulse noise, two special cases have drawn much research interest, that is, salt-and-pepper noise and random-valued noise. Nevertheless, in some applications, such as harsh hydrodynamic experiments, additive white Gaussian noise is introduced as expected during image acquisition, while non-Gaussian noise, especially additive Laplace noise, is also encountered for more accurate modeling transmission in Charge-coupled Device (CCD) channels and interaction between shielding and photons. Accordingly, this paper considers the task of removing mixed Laplace-Gaussian (MLG) noise, where the observation f of an ideal image u is modeled by

$$f(x) = Hu(x) + n(x), x \in U$$

U denotes the image domain, $n(x)$ is regarded as a realization of independent and identically distributed (iid) random variables $Z(x)$, which has the probability density function (PDF)

$$p_z(z; \theta) = \sum_{k=1}^2 \gamma_k p_k(z; \sigma_k^2), \quad (1)$$

where

$$p_1(z; \sigma_1^2) = \frac{1}{2\sigma_1^2} \exp(-|z|/\sigma_1^2),$$

$$p_2(z; \sigma_2^2) = \frac{1}{\sqrt{2\pi\sigma_2^2}} \exp(-|z|^2/2\sigma_2^2)$$

$\theta = \{\theta_1, \theta_2\} = \{\gamma_i, \sigma_i^2, i = 1, 2\}$ is a parameter set, $\gamma_i > 0$ represents the mixture ratio satisfying $\gamma_1 + \gamma_2 = 1$.

Additionally, H can be an identity, blur or projection operator in this paper. The problem of this paper is then to reconstruct u from the observation f with an unknown parameter set θ .

The First-Order Total Variation (FOTV) regularization method, designed originally for Gaussian noise removal, is now one of the most popular approaches for studying inverse problems under various assumptions of noise including Poisson, Speckle, impulse, or even mixed noise. Among the works in the literature, the first-order regularization models given in [6]-[8] are of benefit to our work.

Given the success of FOTV-based models, various modifications have been developed to surmount its artifact, such as the staircase effect and the shortage of smoothness. Among the modifications, we concentrate on the following Higher-Order TV (HOTV) regularization methods. Li, Shen, Fan, Shen [9] proposed the following model

$$\min_u \int_U ((1-g)|\nabla u| + g|\nabla u|^2) dx + \frac{\beta}{2} \int_U (u-f)^2 dx \quad (2)$$

for Gaussian noise removal, where g is a stopping function producing anisotropic diffusion and a weighted fourth-order diffusion equation is derived by steepest descent method. Papafitsoros and Shcönlieb [10] considered the Gauss noise model and the impulse noise model separately, and established a theoretical and numerical framework of the minimization problem

$$\min_u \int_U (\alpha a(|\nabla u|) + \beta b(|\nabla u|^2)) dx + \frac{1}{s} \int_U (Tu - f)^2 dx \quad (3)$$

where $s=1,2$, T is a known linear operator, $\alpha \geq 0, \beta \geq 0$ are regularization parameters, and the convex functions $a(\cdot), b(\cdot)$ have at most linear growth at infinity. They also assured that, by implementing a higher order extension of FOTV, the proposed model can significantly reduce the staircase effect in image restoration.

As mentioned above, the primary goal of this paper is to find an appropriate model for mixed noise removal and image reconstruction. Most existing regularization models have the data fidelity terms determined by the probability distributions of the noises, such as L^2 norm for Gaussian noise and L^1 norm for impulse noise. In applications, however, it is still not well-founded for the noise model, as well as higher-order regularization methods used for hydrodynamic experiments, since the parameters of the PDF are unknown in advance and has to be considered carefully. Moreover, it is not unnecessary to reconsider the assemblage of the punishing functions, and the weighting functions should have been investigated in a more natural and practical

way. In view of that, the problem of image reconstruction is reconsidered and a new framework of the second order regularization method is proposed. Noting that noise modeling is indispensable for image processing and data diagnosing, the first main contribution of this paper is to introduce an applicable calculation method for the parameters of the PDF, which can be generalized to more intricate simulations of real noise. The second contribution lies in designing an efficient and reliable Augmented Lagrange Method (ALM) to solve a constrained minimization problem, where some kind of positive control functions are designed to enhance significant details. The numerical discussion confirms that the proposed model succeeds in avoiding the undesirable pseudo-features in the reconstructed data.

The rest of the paper is organized as follows. In section 2, applying Bayesian inference theory, a new hybrid regularization model is proposed. Furthermore, its algorithm is established with some modification of the ALM. In section 3, some numerical experiments are conducted to prove the applicability of the proposed models. Finally, in section 4, some additional remarks and future work on the model and its algorithm are discussed.

II. MAIN MODEL AND ITS ALGORITHM

A. Mathematical Modeling

The main idea is to configure a regularization model by combing FOTV functionals with HOTV ones through some kinds of weighting functions, intending to enhance true edges and polish fake or insignificant information in the reconstructed images.

By applying the Bayesian inference theory [11] in continuous settings, the maximum a-posteriori probability (MAP) estimator of \mathbf{u} is given by

$$\mathbf{u}^* = \operatorname{argmin}_{\mathbf{u}} \left\{ -\int_U \ln p(\mathbf{f}|\mathbf{u})d\mathbf{x} - \int_U \ln p(\mathbf{u})d\mathbf{x} \right\} \quad (4)$$

It follows from the ideas in [10] that the a priori probability density function, $p(\mathbf{u})$, can be defined by $p(\mathbf{u}) \sim \exp(-R(\nabla\mathbf{u}, \nabla^2\mathbf{u}))$

$$R(\nabla\mathbf{u}, \nabla^2\mathbf{u}) = -\int_U (\alpha|\nabla\mathbf{u}| + \tau|\nabla^2\mathbf{u}|)d\mathbf{x}, \quad (5)$$

where α, τ are positive parameters. On the other hand, by the independency assumption, there holds that

$$p(\mathbf{f}|\mathbf{u}) = p_{\mathbf{z}}(\mathbf{f} - H\mathbf{u}; \theta).$$

We then have a negative log-likelihood functional of the MLG model

$$L(\theta, \mathbf{u}) = -\int_U \left(\ln \left[\frac{\gamma_1}{2\sigma_1^2} \exp\left(-\frac{|f-H\mathbf{u}|}{\sigma_1^2}\right) \right] + \ln \left[\frac{\gamma_2}{2\pi\sigma_2^2} \exp\left(-\frac{|f-H\mathbf{u}|^2}{2\sigma_2^2}\right) \right] \right) d\mathbf{x} \quad (6)$$

The difficulty of computing the minimizer of the functional (6) lies in the log-sum operation. Fortunately, it can be surmounted in the following way. Introduce a vector-valued function $\varphi = \{\varphi_1, \varphi_2\}$ [4], [12] in

$$\Delta_+ = \{\varphi(\mathbf{x}) | 0 < \varphi_1(\mathbf{x}) < 1, \sum_{i=1}^2 \varphi_i(\mathbf{x}) = 1\},$$

and define a functional

$$\mathfrak{N}(\theta, \mathbf{u}, \varphi) = \int_U \sum_{i=1}^2 \varphi_i(\mathbf{x}) [P_1(\mathbf{x}) - \ln Q(\mathbf{x})] d\mathbf{x} + \int_U \sum_{i=1}^2 \varphi_i \ln \varphi_i d\mathbf{x} \quad (7)$$

where

$$P_1(\mathbf{x}) = \frac{|Hu-f|}{\sigma_1^2}, P_2(\mathbf{x}) = \frac{|Hu-f|^2}{2\sigma_2^2}, \\ Q_1(\mathbf{x}) = \frac{\gamma_1}{2\sigma_1^2}, Q_2(\mathbf{x}) = \frac{\gamma_2}{2\pi\sigma_2^2}$$

Then, perform the following iteration scheme

$$\begin{cases} \varphi^{v+1} = \operatorname{argmin}_{\varphi \in \Delta_+} \mathfrak{N}(\theta^v, \mathbf{u}^v, \varphi) \\ (\theta^{v+1}, \mathbf{u}^{v+1}) = \operatorname{argmin}_{\theta, \mathbf{u}} \mathfrak{N}(\theta, \mathbf{u}, \varphi^{v+1}) \end{cases} \quad (8)$$

for given θ^0, \mathbf{u}^0 , where v denotes the inner iteration number.

Utilizing the updating equation

$$\varphi_i^{v+1} = \frac{\gamma_i p_i(H\mathbf{u}^v - f; \theta_i^v)}{\sum_{s=1}^2 \gamma_s^v p_s(H\mathbf{u}^v - f; \theta_s^v)}, i = 1, 2 \quad (9)$$

it can be proven that the above scheme leads to the same global minimize of $L(\theta, \mathbf{u})$.

Thus, we turn to consider the following minimization problem (MLG-TV BH)

$$\min_{\theta, \mathbf{u}} E(\theta, \mathbf{u}) = \mathfrak{N}(\theta, \mathbf{u}, \varphi^{v+1}) + R(\nabla\mathbf{u}, \nabla^2\mathbf{u}). \quad (10)$$

B. Proposed algorithm of MLG-TV BH

The algorithm for MLG-TV BH is based on the variable splitting method and the ALM, where penalty parameters in the quadratic infeasibility terms of ALM are replaced by adaptively selective functions. Indeed, reuse the pattern of (8) and split (10) into several minimization sub-problems. Use v to denote the iteration number. θ^0 is a coarse guess of the parameters θ , then the minimizer $(\theta^{v+1}, \mathbf{u}^{v+1})$ are given by

$$\begin{cases} \mathbf{u}^{v+1} = \operatorname{argmin}_{\mathbf{u}} E(\theta^v, \mathbf{u}) \\ \theta^{v+1} = \operatorname{argmin}_{\theta} E(\theta, \mathbf{u}^{v+1}) \end{cases} \quad (11)$$

iteratively.

In terms of calculating θ^{v+1} , it yields by direct computation that

$$(\sigma_1^2)^{v+1} = \frac{\int_U \varphi_1^{v+1} |Hu^{v+1} - f| d\mathbf{x}}{\int_U \varphi_1^{v+1} d\mathbf{x}}, (\sigma_2^2)^{v+1} = \frac{\int_U \varphi_2^{v+1} |Hu^{v+1} - f|^2 d\mathbf{x}}{\int_U \varphi_2^{v+1} d\mathbf{x}}, \quad (12)$$

$$\gamma_1^{v+1} = \int_U \frac{\varphi_1^{v+1} d\mathbf{x}}{|U|}, \gamma_2^{v+1} = 1 - \gamma_1^{v+1}, |U| = \int_U 1 d\mathbf{x} \quad (13)$$

As for the \mathbf{u} -minimization problem of (11), it can be proven that there exists a unique solution in the space of bounded Hessian (BH) [10], the details of which are omitted in this paper.

To circumvent the non-differentiability of the L^1 norm arisen in our model, a modification of the Alternating Direction Augmented Lagrangian (ADAL) method [13][14] is proposed, as follows.

Firstly, introduce auxiliary vector-valued variables q, h , and split the minimization problem into

$$\min_{\mathbf{u}, q, h} \mathfrak{N}(\theta^v, \mathbf{u}, \varphi^{v+1}) + \int_U (\alpha|q| + \tau|h|)d\mathbf{x} \quad \text{subject to} \\ q = \nabla\mathbf{u}, h = \nabla^2\mathbf{u}.$$

Secondly, configure an alternating minimization process. More specifically, use a third variable k to approximate the fidelity term $H\mathbf{u} - f$, and introduce spatially detail selective functions $\rho_k(\mathbf{x})$, $\rho_q(\mathbf{x})$, $\rho_h(\mathbf{x})$, and then consider the following functional

$$I^p(\mathbf{u}, k, q, h; \mu) = S(k) + \langle \mu_k, H\mathbf{u} - f - k \rangle + \int_U \alpha|q|d\mathbf{x} +$$

$$\begin{aligned} & \frac{1}{2} \int_U \rho_k(x) |Hu - f - k|^2 dx + \langle \mu_n, \nabla u - q \rangle + \\ & \frac{1}{2} \int_U \rho_q(x) |\nabla u - q|^2 dx + \int_U \tau |h| dx + \langle \mu_h, \nabla^2 u - h \rangle + \\ & \frac{1}{2} \int_U \rho_h(x) |\nabla^2 u - h|^2 dx \end{aligned}$$

where $S(Hu - f) = \mathfrak{N}(\theta^v, u, \varphi^{v+1})$, $\rho = (\rho_k, \rho_q, \rho_h)$ is the vector of positive penalty functions to be specified latter, $\mu = (\mu_k, \mu_q, \mu_h)$ is the vector of Lagrange multipliers.

Given initial values u^0, k^0, q^0, h^0 . If u^v, k^v, q^v, h^v are the current approximation to the multiplier vector, the fidelity term, the gradient and the Hessian of the original data, then we turn to consider the following problems

$$\text{SP1: } u^{v+1} = \operatorname{argmin}_u L^\rho(u, k^v, q^v, h^v; \mu^v) \quad (14)$$

$$\text{SP2: } k^{v+1} = \operatorname{argmin}_k L^\rho(u^{v+1}, k, q^v, h^v; \mu^v) \quad (15)$$

$$\text{SP3: } q^{v+1} = \operatorname{argmin}_q L^\rho(u^{v+1}, k^{v+1}, q, h^v; \mu^v) \quad (16)$$

$$\text{SP4: } h^{v+1} = \operatorname{argmin}_h L^\rho(u^{v+1}, k^{v+1}, q^{v+1}, h; \mu^v) \quad (17)$$

$$\text{SP5: } \mu^{v+1} = \operatorname{argmax}_\mu L^\rho(u^{v+1}, k^{v+1}, q^{v+1}, h^{v+1}; \mu) \quad (18)$$

For the minimization problem (14), which is a quadratic problem, by a routine computation, it yields the following fourth-order Euler-Lagrange equation

$$-\operatorname{div}(\rho_q \nabla u) + \operatorname{div}^2(\rho_h \nabla^2 u) + W(u, f) = 0 \quad (19)$$

$$\begin{aligned} W = \operatorname{div}(\rho_q q^v - \mu_q) - \operatorname{div}^2(\rho_h h^v - \mu_h) + \\ H^s(\rho_k(Hu - f - k^v) + \mu_k^v) \end{aligned} \quad (20)$$

with boundary conditions

$$\partial u / \partial N = \nabla u_x \cdot N = \nabla u_y \cdot N = 0$$

$$\langle \nabla \cdot (\rho_n \nabla u_x), n_1 \rangle = \langle \nabla \cdot (\rho_n \nabla u_y), n_2 \rangle = 0.$$

where $N = (n_1, n_2)$ is the outward unit normal vector to the boundary, H^s is the adjoint operator of H .

For the problem (15), combine it with the updating of μ_k in (18). Introduce an auxiliary variable m to approximate $Hu^{v+1} - f - k$, utilize the dual method, we find that the maximize μ_k^{v+1} fulfills

$$\frac{\mu_k^{v+1}}{\rho_k(x)} - \frac{\mu_k^v}{\rho_k(x)} = Hu^{v+1} - f - k^{v+1} \triangleq g.$$

Detonate $A(x) = \varphi_1^{v+1} / (\sigma_1^2)^v$, $B(x) = \varphi_2^{v+1} / (\sigma_2^2)^v$, consider $\delta M(k) / \delta k = 0$, where

$$M(k) = S(k) + \frac{1}{2} \int_U \rho_k \left(Hu^{v+1} - f - k + \frac{\mu_k^v}{\rho_k} \right)^2 dx,$$

there holds the following iteration scheme for solving (15):

$$\begin{cases} k^{v+1} = \frac{\rho_k}{B + \rho_k} \operatorname{shrink}(g, \frac{\rho_k}{A}), \\ \frac{\mu_k^{v+1}}{\rho_k(x)} - \frac{\mu_k^v}{\rho_k(x)} = g. \end{cases} \quad (21)$$

In a similar way, the minimization problem (16), (17) can be solved. Indeed, there have

$$\begin{cases} q^{v+1} = \operatorname{shrink}\left(\nabla u^{v+1} + \frac{\mu_q^v}{\rho_q(x)} \frac{\rho_q(x)}{\alpha(x)}\right), \\ \frac{\mu_q^{v+1}}{\rho_q(x)} - \frac{\mu_q^v}{\rho_q(x)} = \nabla u^{v+1} - q^{v+1} \end{cases}, \quad (22)$$

and

$$\begin{cases} h^{v+1} = \operatorname{shrink}\left(\nabla^2 u^{v+1} + \frac{\mu_h^v}{\rho_h(x)} \frac{\rho_h(x)}{\tau(x)}\right), \\ \frac{\mu_h^{v+1}}{\rho_h(x)} - \frac{\mu_h^v}{\rho_h(x)} = \nabla^2 u^{v+1} - h^{v+1} \end{cases}, \quad (23)$$

In summary, an alternating minimization algorithm of the MLG-TVBH model is given as follows.

Algorithm Given a tolerance $\epsilon_0 > 0$. Choose initial guess $u^0, k^0 = \mu_k = 0, q^0 = \mu_q = 0, h^0 = \mu_h = 0, \theta^0$.

Set $v = 0$, do

Step 1. Calculate φ^{v+1} by equation (9).

Step 2. Calculate u^{v+1} by (19), (20).

Step 3. Calculate $k^{v+1}, q^{v+1}, h^{v+1}$ and $\mu_k^{v+1}, \mu_q^{v+1}, \mu_h^{v+1}$ by (21)-(23), respectively.

If $|u^{v+1} - u| / |u^v| \leq \epsilon_0$, end the recurrence. Otherwise, go to the next steps.

Step 4. Calculate θ^{v+1} by (12), (13).

Step 5. Set $v = v + 1$, go to step 1.

It can be seen that only step 2 is time-consuming, while the others can be calculated explicitly.

III. APPLICATIONS

In this section, the proposed method is applied for image denoising with H representing the identity operator and data reconstruction with H representing the Abel transform [15] [16], i.e.,

$$Hu(x, y) = 2 \int_{|z|}^T \frac{ru(x, y)}{\sqrt{x^2 - z^2}} dz. \quad (24)$$

The intensity of the observed image is rescaled to the interval [0,1] before operation. Some synthetic images are utilized, and degenerated versions are obtained by adding random noise to the clean ones with certain proportion. The programs were coded in C++ and run on a personal computer with four 2.83 GHz CPU processors.

A. Configuration of ρ

Based on the ideas in [9][16], the second-order total variation is used to restrain the staircase effect in the restored images. Meanwhile, the strictly positive penalty functions ρ_q, ρ_h , and ρ_k act as stopping functions preventing from over-blurring. The stopping functions can be defined by

$$\begin{aligned} \rho_q &= 1 / \sqrt{1 + (|\nabla G_{\sigma_0} * u| / K_q)^2}, \\ \rho_h &= 1 / \left(\sqrt{1 + (|\nabla G_{\sigma_0} * u| / K_h)^2} \right)^3, \end{aligned}$$

and

$$\rho_k(x) = \exp(-\rho_q(x)),$$

respectively, where G_{σ_0} is the Gaussian filter with fixed parameter σ_0 , '*' denote the convolution operator. In application, K_q, K_h are positive value with $K_q \gg K_h$. The former is the value of true edges in the original image, and the other is used to distinguish pseudo signal caused by the staircase effect.

B. The numerical scheme for (19)

It is noted that there have been many approaches of computing u in the literature, such as steepest descent method (e.g., [17]), lagged-diffusivity fixed-point method (e.g., [18]), additive operator splitting (AOS, e.g., [19], [20]), dual method (e.g., [21]), and so on.

In this paper, the gradient descent method and the semi-implicit AOS scheme are utilized to get the solution of (19). Intuitively, in homogeneous regions of a given image, $|\nabla^2 \mathbf{u}|$ is significantly smaller than $|\nabla \mathbf{u}|$, and thus, integrate the fourth-order divergence term into the source term \mathbf{W} , and consider the following evolution equation

$$\mathbf{u}_t - \operatorname{div}(\rho_q \nabla \mathbf{u}) = -\operatorname{div}^2(\rho_h \nabla^2 \mathbf{u}) - \mathbf{W}(\mathbf{u}, f) \quad (25)$$

with initial-boundary conditions. It can be seen that the stopping functions ρ_q, ρ_h are fundamental in our method, since isotropic diffusion is undesired as they are spatially invariable.

To meet the boundary condition, we utilize the trick of continuous extension to the boundary of original images. The scale derivative term, i.e., \mathbf{u}_t , is approximated by a forward difference scheme. The first-order divergence term is approximated by the standard central difference, and the second-order divergence term is approximated by finite forward and/or backward differences (e.g., [9]). Hence, equation (25) can be solved by a semi-implicit AOS scheme, which can be used to deal with the heat flow equation to compute the Gaussian convolution.

Additionally, to assess the reconstruction performance, the quality index of restoration

$$\text{PSNR} = 10 \lg \left(255^2 / \frac{1}{F_h F_v} \sum_{i,j=1}^{F_h F_v} (u_{i,j} - f_{i,j})^2 \right) \quad (26)$$

is adopted in this paper.

C. Initial value and parameter selection

In applications, we pay more attention is the selection of parameters $(\sigma_i^2)^0, i = 1, 2$ and the valve value K_q than the other parameters, such as K_h, α, τ and the scale step size ($\equiv 0.1$), since they are less sensitive and almost consistent in our experiments. For example, in this paper, $\alpha = 2, \tau = 0.1$, and $K_h = 10^{-4}$. The stopping criterion in our experiments is $\epsilon_0 = 10^{-4}$. In this paper, $\gamma_1^0 = \gamma_2^0 = 0.5, (\sigma_1^2)^0 = 0.5, (\sigma_2^2)^0 = 0.1 \sim 0.05$.

D. Image denoising

In this section, some experiments of the proposed model are listed for reconstructing images corrupted by different kinds of mixed noise.

Figure 1 shows an experiment of removing mixed Lapla ce-Gaussian noise. Figure 1A) is a synthesized image according to [10], Figure 1B) is a degenerated version of Figure 1A) with PSNR =26.45dB by adding 30% Laplace noise ($\sigma_1^2 = 0.05$) and Gaussian noise ($\sigma_2^2 = 0.05$) to Figure 1A). Figure 1C) is a recovered image using our proposed model, PSNR=33.07dB, $K_q = 0.03$.

Figure 2 presents another experiment. Figure 2A) is a synthesized image composed of two triangles and one circle. Figure 2B) is obtained by adding Laplace-Laplacian noise to

Figure 2A) with PSNR=19.61dB. Figure 2C) is recovered by the proposed model with PSNR=36.25dB, $K_q = 0.045$.

Figure 3 shows the validation of mixed Gaussian noise removal. Figure 3A) is the standard Lenna image. Figure 3B) is a noisy image of Figure 3A) by additive Gaussian noise with PSNR=19.29 dB. Figure 3C) is obtained by our proposed method with PSNR=10.18dB.

E. Object reconstruction

In this section, we give only one experiment on the France Test Object (FTO).

In Figure 4, Figure 4A) is the original image of its density distribution. Figure 4B) is its projection image, which is corrupted by mixed Laplace ($\sigma_1^2 = 0.03, 30\%$) and Gauss ($\sigma_2^2 = 0.005$) noise. Figure 4C) is a reconstructed image of Figure 4B) using the Abel inversion formula (e.g., [15]). Figure 4D) is a reconstructed version obtained by our proposed method with parameters $\alpha = 1.5, \tau = 0.2, K_q = 0.015, K_h = 0.0002$.

IV. CONCLUSIONS AND REMARKS

In this paper, a new modeling framework is proposed, which is based on the assumption of mixed Laplace-Gaussian noise. The proposed model can be seen as an improvement of some known works, such as those in [8]-[10].

The algorithm of the proposed model is also investigated via the splitting tactics and the ALM with some modification. Spatially adaptive functions are introduced to enhance significant information in the original images. Also, a new soft shrinking formula is obtained. Numerical experiments illuminate its validation of recovering images in the presence of varies kinds of mixed noise.

The proposed model can be further extended to process images degenerated by blur and inhomogeneous light field, which is to be discussed in future work.

REFERENCES

- [1] B. Zhang, M. J. Fadili, J. I. Starck, "Multiscale variance-stabilizing transform for mixed-Poisson-Gaussian processes and its application in bioimaing," IEEE Interational Conference on Image Processing, 2007, pp. 233-236.
- [2] A. Foi, M. Trimeche, K. Eqiazarian, "Practical Poissonian-Gaussian noise modeling and fitting for single-image raw-data," IEEE Trans. Image Processing, 2008, vol. 17, pp. 1737-1754.
- [3] J. F. Cai, R. Chan, M. Nikolova, "Two-phase methods for deblurring images corrupted by impulse plus gaussian noise," Inverse Problem Imaging, 2008, vol. 2, pp. 187-204.
- [4] J. Liu, X.-C. Tai, H.-Y. Huang, Z.-D. Huan, "A weighted dictionary learning model for denoising images corrupted by mixed noise," IEEE Trans. Image Processing, 2013, vol. 22(3), pp. 1108-1120.
- [5] J. Delon, A. Desolneux A, "A patch-based Approach for removing impulse or mixed Gaussian-impulse noise," SIAM J. Imaging Sciences, 2013, vol. 6(2), pp. 1140-1174.
- [6] J. Liu, H.-Y. Huang, Z.-D. Huan, H.-L. Zhang, "Adaptive variational method for restoring color images with high

density impulse noise,” *Inter. J. Comput. Vis.*, 2010, vol. 90, pp. 131-149.

[7] M. Hintermüller, A. Langer, “Subspace correction methods for a class of nonsmooth and nonadditive convex variational problems with mixed L^1/L^2 data fidelity in image processing,” *SIAM J. Imaging Sci.*, 2013, vol. 6(4), pp. 2134-2173.

[8] Z.Gong, Z. Shen, K. C. Toh, “Image restoration with mixed or unknown,” *Multiscale Model. Simul.*, 2014, vol.12(2), pp. 458-487.

[9] F. Li, C.-M. Shen, J. Fan, C.-L. Shen, “Image restoration combining a total variational filter and a fourth-order filter,” *J. Vis. Commun. Image R.*, 2007, vol. 18, pp. 322-330.

[10] K. Papafitsoros, C.B. Schönlieb, “A combined First and second order variational approach for image reconstruction,” *J. Math. Imaging Vis.*, 2014, vol. 48, pp. 308-338.

[11] J. Idier, Bayesian approach to inverse problems. Wiley, New York, 2008.

[12] J.Liu, H.-L. Zhang, “Image segmentation using a local GMM in a variational framework,” *J. Math. Imaging Vis.*, 2013, vol.46, pp. 161-176.

[13] D. P. Bertsekas, J. N. Tsitsiklis, “Parallel and distributed computation: numerical methods,” Athena Scientific, Belmont, Massachusetts, 1997.

[14] V. P. Gopi, P. Palanisamy P, K. A. Wahid, “Micro-CT image reconstruction based on alternating direction augmented Lagrangian method and total variation,” *Comput. Medical Imaging Graph.*, 2013, vol. 37, pp. 419-429.

[15] R. Abraham, M. Bergounioux, E. Trélat, “A penalization approach for tomographic reconstruction of binary axially symmetric objects,” *Appl. Math. Optim.*, 2008, vol.58, pp. 345-371.

[16] R. H. Chan, H. Liang, S. Wei, M. Nikolova, X.C. Tai, “High-order total variation regularization approach for axially symmetric object tomography from a single radiograph,” *Inverse Problems & Imaging*, 2015, Vol.9(1), pp. 55-77.

[17] A. Chambolle, P. L. Lions, “Image recovery via total variation minimization and related problems,” *Numer. Math.*, 1997, vol.76, pp. 167-188.

[18] M. Lysaker, X.-C. Tai, “Iterative image restoration combining total variation minimization and a second-order functional,” *Int. J. Comput. Vis.*, 2006, vol.66(1), pp. 5-18.

[19] T.-T. Wu, Y.-F. Yang, Z.-F. Pang, “A modified fixed-point iterative algorithm for image restoration using fourth-order PDE model,” *Applied Numer. Math.*, 2012, vol. 62, pp. 79-90.

[20] T. Lu, P. Neittaanmaki, and X.-C. Tai, “A parallel splitting up method and its application to Navier-Stokes equations,” *Applied Mathematics Letters*, 1991, vol.4(2), pp. 25-29.

[21] J. Weickert, B. ter Haar Romeny, and M. Viergever, “Efficient and reliable schemes for nonlinear diffusion filtering,” *IEEE Trans. Image Proc.*, 1998, vol.7, pp. 398-410.

[22] A.Chambolle, T. Pock, “A first-order primal-dual algorithm for convex problems with applications to imaging,” *J. Math. Imaging Vis.*, 2011, vol.40(1), pp. 120-145.

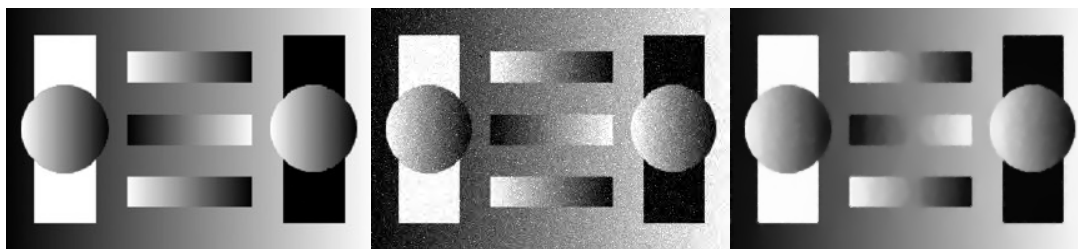


Figure 1. A) (Left) An synthesized noise-free image[10]; B) (Center) Mixed Gaussian-Laplacian noise added to A); C) (Right) Restored version by our model.

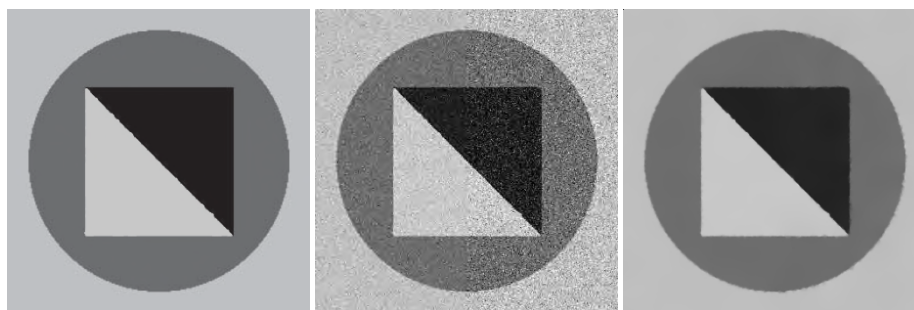


Figure 2. A) (Left) A synthesized image; B) (Center) Mixed Laplacian-Laplacian noise ;C) (Right) A restored version using our proposed model.



Figure 3. A) (Left) Lenna image; B) (Center) A noisy version of A) by adding mixed Gaussian noise; C) (Right) A restored version obtained by our proposed method

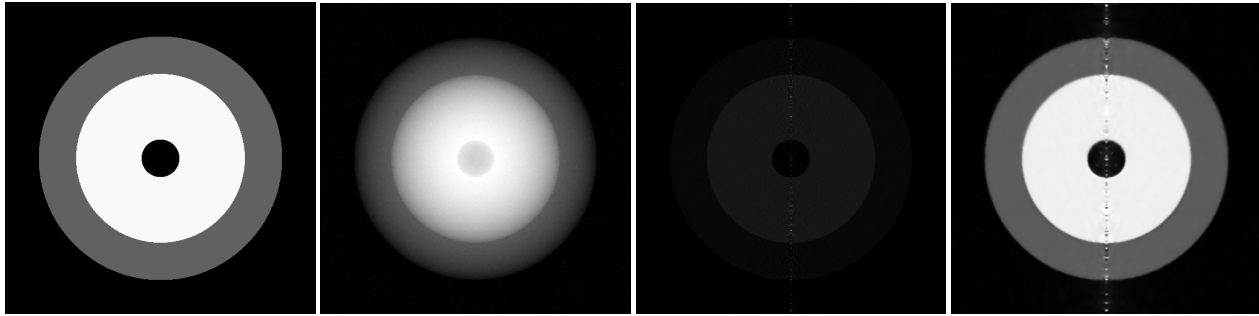


Figure 4. A) (Left) The original density distribution image of FTO; B) (MidLeft) A degenerated image of the projection of A), obtained by utilizing the Abel formulation (20) firstly, and then adding mixed Laplace-Gauss noise. C) (MidRight) A reconstructed image of B) using the Abel Inverse formula [15] D) (Right) A reconstructed image using our proposed method.